

Research Journal of Pharmaceutical, Biological and Chemical Sciences

Investigating the Effect of Incorporating Nanosilver/Nanohydroxyapatite with Blend of (PAAc-Cs) on the Shear Bond Strength of Human Bone.

E M Abdelrazek¹, A M Hezma^{2*}, N El-sheshtawy¹, S Elbeltagy³ and A El-Khodary¹.

¹Physics Department, Faculty of Science, Mansoura University, Mansoura, Egypt.

²Spectroscopy Department, Physics Division, National Research Centre, Dokki, Giza, Egypt.

³Canadian international collage CIC elshekh zayd campus, 6 October City, Egypt.

ABSTRACT

Nano-particles hydroxyapatite (HA) was prepared via an in-situ biomimetic process with polyacrylic acid (PAAc) and chitosan (Cs) as a host polymeric material with organic/inorganic ratio 60/40 wt%. Silver nitrate with different concentrations was added to improve the physical properties and bioactivity of the biocomposite. Fourier transform infrared spectroscopy (FTIR), transmission electron microscopy (TEM), scanning electron microscopy (SEM), and X-ray diffraction (XRD), were used to test the physical and chemical characteristics of biocomposites. Kinetic parameters were determined from the weight loss data using non isothermal Thermogravimetric Analysis (TGA) and also the main decomposition temperatures and the main degradation step were describes and discussed. The SBF incubation test confirmed that the fast formation of apatite-like materials suggests in vitro bioactive behavior of the biocomposite, possibly due to the addition of metallic Ag nanoparticles. This study demonstrated that Ag nanoparticles in HA/PAAc-Cs-Ag biocomposite activates bioactivity and supports growth of apatite-like materials. Thus the resulting new materials are hoped to be applicable in the biomedical fields.

Keywords: Biocomposites; FTIR; X-ray; TGA; TEM; SEM

**Corresponding author*

INTRODUCTION

Hard tissue repair or regeneration is a common yet complicated clinical problem in orthopaedic surgery. Bone tissue engineering substitutes is one of the best choice for treating bone defects, because it has been heralded as the alternative strategy to regenerate bone [1]. The development of biomimetic materials has long been a major goal in the field of bone tissue engineering. Natural bone is a complex inorganic-organic nanocomposite material, in which hydroxyapatite (HA, $\text{Ca}_{10}(\text{PO}_4)_6(\text{OH})_2$) nanocrystallites and collagen fibrils are well organized into hierarchical architecture over several length scales [2, 3]. Thus, the main idea to get artificial biomaterials [4] as bone substitutes in biomimetic inspired approaches is to produce nanocrystallites of calcium phosphate (CaP) salts such as hydroxyapatite dispersed into polymer matrices.

Thus, the good bone compatibility of HA makes it suitable for the repair or replacement of damaged or diseased bone. However, the poor mechanical and fatigue properties limit its applicability to the low load bearing areas of human skeleton. In addition to this, sintered HA is extremely hard and brittle which makes its processing difficult. It has been reported that HA in the form of powders, used for the treatment of bone defects, has problem associated with migration to places other than implanted sites [5, 6]. Hence composite materials of HA with organic polymers, that can to certain extent reduce the above problems, have become of great interest [7]. A wealth of research has been carried out in this regard and composite materials based on HA and a variety of polymers have been reported [8]. Chitosan, a cationic polysaccharide, is a (1,4) linked 2-amino-2-deoxy-D glucan and can be prepared by the N-deacetylation of chitin. Chitosan has both reactive amino and hydroxyl groups that can be used to chemically alter its properties under mild reaction conditions. Therefore, there have been many interesting chitosan derivatives for the biomedical applications [9, 10]. Efforts for the development of bone graft materials based on chitosan–calcium phosphate and chitosan–HA were made by several research groups [5, 11, 12]

Therefore, it is desirable to develop a composite material with favorable properties of chitosan and hydroxyapatite. The designed composites are expected to show increased osteoconductivity and biodegradation together with sufficient mechanical strength, which will be of great importance for bone remodeling and its growth.

Polyacrylic acid is a water soluble and biocompatible polymer and has been extensively studied in the context of biomedical applications [13-15]. The bioactivity of any biocomposite materials can be attributed to the formation of a biologically active bone-like carbonate containing apatite layer. Also, the incorporation of functional nanoparticles as Ag nanoparticles into biocomposite materials can also be achieved by simple convenient chemical preparation method. Whilst the resulting biocomposite exhibit the distinctive properties of the incorporated nanoparticles such as increasing the bioactivity of the biocomposite can even be expected over those without nanoparticles.

In this study, we performed comparative analyses of HA/PAAc-Cs-Ag nanoparticles biocomposite prepared by *in-situ* precipitation method [16] before and after incubation in stimulated body fluid (SBF). Furthermore, the influence of Ag nanoparticles in terms of apatite formation in the biocomposite surface was examined. The structural, thermal and bioactivity properties were studied before and after incubation in SBF solution.

EXPERIMENTAL WORK

Materials

The chemicals used were Polyacrylic Acid (PAAc), $w_x=35\%$ solution in water with $M_w=100,000$ from Aldrich (Lot No. 523,925), Chitosan (Cs) low molecular weight from Aldrich (75-85% deacetylated), Calcium Nitrate A.R ($\text{Ca}(\text{NO}_3)_2 \cdot 4\text{H}_2\text{O}$) from WINLAB, UK (Lot No. 121,065), Silver Nitrate (AgNO_3) and Diammonium Hydrogen Phosphate ($(\text{NH}_4)_2 \cdot \text{HPO}_4$) from SISCO Research Laboratories pvt. LTD, India (Lot No. 0149,174). All chemicals were used as received.

Preparation of biocomposite using in situ method

For Preparation of PAAc/Cs-HA biocomposite we use the following procedures; certain amount of PAAc was dissolved in double distilled water to obtain solution of PAAc. Then, the same amount of Cs solution

was prepared by dissolving Cs in of acetic acid solution (2 vol.%) with stirring at room temperature for 24 h to get a perfectly transparent solution. The two solutions were added to each other to form a PAAc/CS blend with 50/50wt%. Calculated amount of calcium nitrate ($\text{Ca}(\text{NO}_3)_2 \cdot 4\text{H}_2\text{O}$) was dissolved in bidistilled water with vigorous stirring (2 h) to form 0.5 M/L. The pH was adjusted at about 10 by adding drop by drop NH_4OH at constant stirring in room temperature. $(\text{NH}_4)_2\text{HPO}_4$ solution was added drop by drop at the same pH with stirring for 7 hours until turbidity appears in the solution due to the formation of amorphous calcium phosphate[16]. The inorganic/organic ratios were adjusted at (60/40) wt%. During preparation different concentration from silver nitrate were added to the composite as shown in table(1). Silver nitrate was added to the polymer solution before addition of HA to test the size of silver particles by TEM. After formation of HA, the final powders were compressed as tablets of 10mm diameter and 5mm height and characterized for their physico-mechanical characteristics.

Table 1: The samples concentrations

| Sample before SBF (S samples) | Sample after SBF (B samples) | PAAc | Cs | HA | AgNO ₃ |
|-------------------------------|------------------------------|------|----|----|-------------------|
| S ₀ | B ₀ | 20 | 20 | 60 | 0 |
| S _{0.1} | B _{0.1} | 20 | 20 | 60 | 0.1 |
| S _{0.2} | B _{0.2} | 20 | 20 | 60 | 0.2 |
| S _{0.4} | B _{0.4} | 20 | 20 | 60 | 0.4 |
| S _{0.8} | B _{0.8} | 20 | 20 | 60 | 0.8 |

Experimental analysis

Fourier Transform Infrared Spectrophotometer (FT-IR) measurements were carried out using the single beam (FT-IR-400, JASCO, Japan) in the spectral range of 4000–400 cm^{-1} at room temperature with scanning speed of 2 $\text{mm} \cdot \text{s}^{-1}$. FT-IR measurements were used to determine the bonding between the inorganic phase and organic phases.

X-ray diffraction analysis were studied by using DIANO corporation-USA equipped with Cu $K\alpha$ radiation at $\lambda = 1.5406 \text{ \AA}$, the Bragg angle (2θ) in the range of 4–70°, step size = 0.02 and step time 0.4s at room temperature. The morphology of the films was characterized by scanning electron microscopy using (JEOL 5300, Tokyo, Japan), operating at 30 KV accelerating voltage. Surface of the samples were coated with a thin layer of gold (3.5 nm) by the vacuum evaporation technique to minimize sample charging effects due to the electron beam. The Ca/P ratio was determined by EDX analysis from SEM.

A Shimadzu TGA-50H was used for the thermogravimetric analysis of the samples. A small amount (4 – 10 mg) of the sample was taken for the analysis and the samples heated from room temperature to 800°C at a rate of 10 °C/min in nitrogen atmosphere in platinum cell. Transmission electron microscopy (TEM) was employed to detect the morphology of the HA nanoparticles and that in composite particles. TEM observation and the corresponding selected area electron diffraction were performed on a JEOL JEM-1230 electron microscope at accelerating voltage of 150 kV.

RESULT AND DISCUSSION

Transmission electron microscope (TEM)

Figure 1. Shows that silver nanoparticles are spherical in shape having smooth surface and are well dispersed. The average diameter of silver nanoparticles of diameters around 35 nm. TEM image also shows that the produced nanoparticles have less narrow size distribution[17]

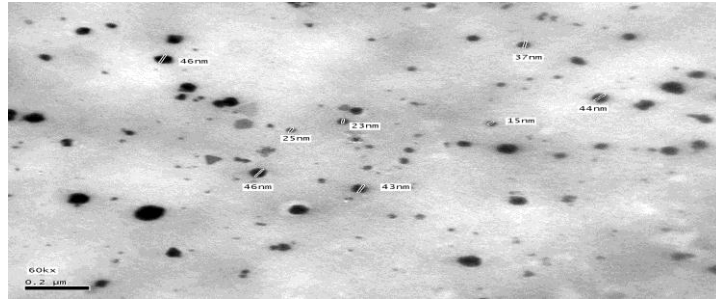


Figure 1. TEM images of Ag nanoparticles

Scanning Electron microscope (SEM)

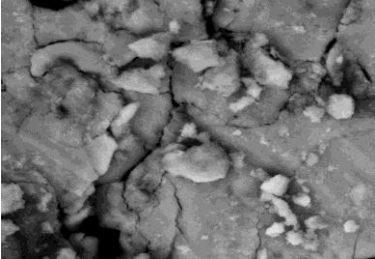
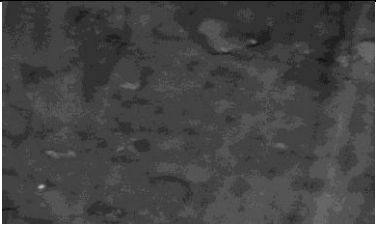
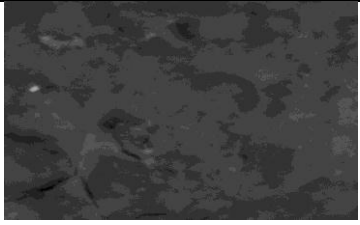
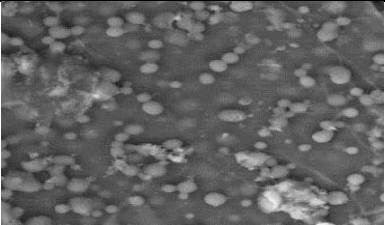
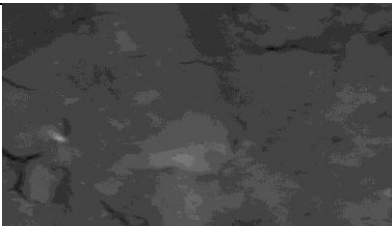
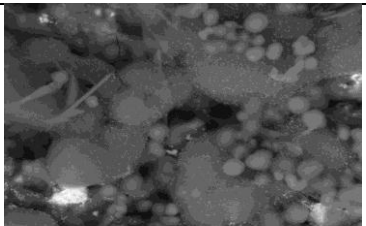
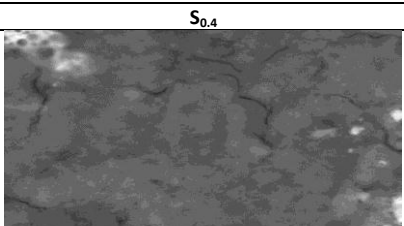
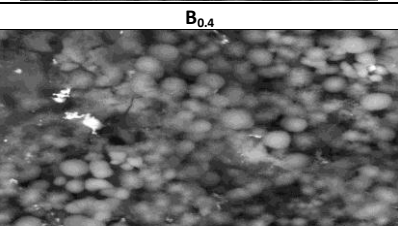
| (a) | (b) |
|---|--|
|  |  |
| S_0 | B_0 |
|  |  |
| $S_{0.1}$ | $B_{0.1}$ |
|  |  |
| $S_{0.2}$ | $B_{0.2}$ |
|  |  |
| $S_{0.4}$ | $B_{0.4}$ |
|  |  |
| $S_{0.8}$ | $B_{0.8}$ |

Figure 2: FE-SEM images of biocomposite samples with different concentrations of silver nitrate a) before and b) after soaking in SBF solution

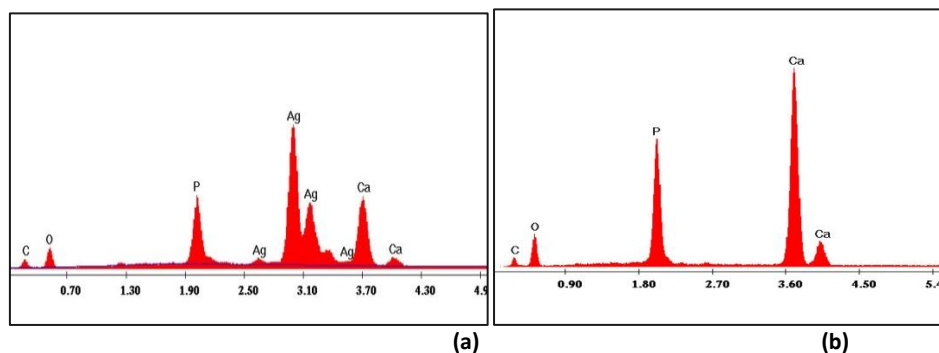


Figure 3: EDX analysis for (a) $S_{0.8}$ sample (b) $B_{0.8}$ sample

FE-SEM (Fig.2) spectrum of S and B samples, are shown. The morphology of biocomposites before and after soaking in SBF was investigated by SEM. From the images mineral crystals were observed to grow on all B biocomposites samples after 14 days immersion in SBF. Fig. 2 (B samples) show that after immersion for 14 days, the apatite crystals covered the samples increased with increasing Ag nanoparticles percent and reach to cover the most regions of sample $B_{0.8}$ surface. In addition, nucleation of new mineral particles are in the form of spherical shape after immersion in SBF.

The phase and composition analyses of the prepared samples (S samples) and the precipitated crystals reveal that these crystals are apatite and are similar to the mineral phase of the bone. These observations indicated that the mineral layer was formed continuously on the surface of the composite and that the composite containing relatively larger amount of Ag nanoparticles had greater ability to induce the formation of minerals *in vitro*. To confirm the presence of HA and the formation of apatite-like materials in the polymer mats after immersion into SBF solution, we performed the SEM-EDX analysis (Fig.3).EDX spot analysis confirmed phosphorus and calcium to be present in the surface of $S_{0.8}$ sample (Fig. 3a) with Ca/P molar ratio of about 1.68 and suggest that the doping Ag^+ has little influence on the morphology of the HA. EDX spot analysis for $B_{0.8}$ samples (Fig. 3b) confirm of the formation of apatite-like materials on biocomposite surface after immersion into SBF solution with Ca/P molar ratio about 1.67. It is known that Ca/P ratio in human bone is 1.67[18].

Fourier transforms infrared analysis (FT-IR)

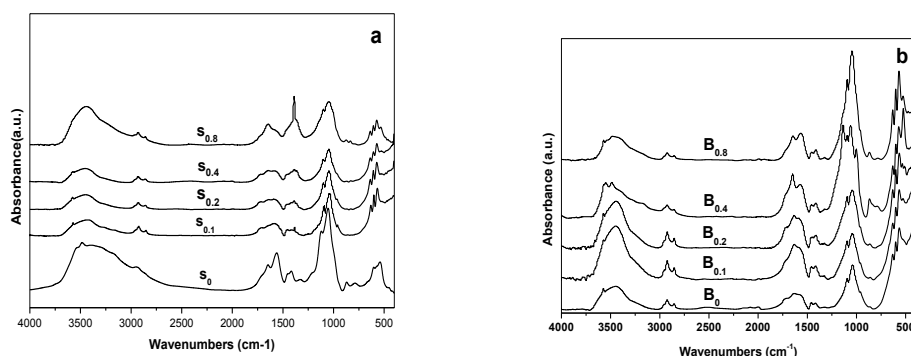


Figure 4: FT-IR absorption spectra of biocomposite samples with different concentrations of silver nitrate a) before (S samples) and b) after soaking in SBF solution (B samples)

Figure 4.a shows FT-IR absorption spectra of the PAAc/Cs-HA biocomposite with inorganic/organic ratio 60/40wt% with different concentrations of silver nitrate (0.1, 0.2, 0.4 and 0.8gm) recorded at the room temperature in the spectral region 4000-400 cm^{-1} . For IR spectrum of PAAc/Cs-HA the characteristic absorption band between 2800 and 3700 cm^{-1} is attributed to the OH stretch of $Ca(OH)_2$, HA and NH stretch of NH_4^+ from $(NH_4)_2.HPO_4$ [19, 20]. The PO_4^{3-} stretching mode is positioned at 1031 cm^{-1} as a main sharp band. There are other bending modes of PO_4^{3-} at 602 and 563 cm^{-1} . The small band at 874 cm^{-1} is also assigned to NO_3^- bending mode [19-23]. The characteristic peak observed at 1626 cm^{-1} can be assigned to the NH_3^+ absorption band of Cs [24]. Furthermore, the absorption peaks at 1538 and 1404 cm^{-1} could be assigned to asymmetric

symmetric stretching vibrations of COO^- anion groups. These results indicated that the carboxylic groups of PAAc were dissociated into COO^- groups, which complexed with protonated amino groups of Cs through electrostatic interaction to form the polyelectrolyte complex during the polymerization and chelate with Ca atoms present on surface of HA nano-particles in-situ [21, 25, 26].

In addition, the stretching vibration at 3414 corresponding to OH/NH_2 groups has shifted to 3424 cm^{-1} , indicating that the silver particles are bounded to the functional groups present both in chitosan and PAAc. The shifting of the peak is due to formation of co-ordination bond between the silver atom and the electron rich groups (oxygen/nitrogen) present in chitosan[27]. This causes an increase in bond length and frequency. All the above observations found in the FT-IR spectra of powder confirm the presence of silver nanoparticles in the chitosan-PAAc blend.

After immersion in SBF solution for 14 days very strong bands vibration mode of the phosphate group were observed, which belongs to the bone-like apatite of vibrational bands of carbonate groups. They were band at $770, 1419$ and 1529 cm^{-1} corresponding to CO_3^{2-} ions present in the apatite structure [28-30], as shown in Fig. 4b. These results suggested that the apatite formed on the surface of composite in SBF was carbonated apatite, which is similar in composition and structure to bone apatite [31]. After incubation in the SBF solution we can observe that the intensity of absorbance band increased in case of presence of Ag nanoparticles in the biocomposites this cases increase the bioactivity which required for the biomaterials used.

X-Ray Diffraction analysis (XRD)

Fig. 5 (a) and (b) show the XRD patterns of the biocomposite samples before and after soaking in SBF solution, respectively. As shown by the XRD pattern in Fig. 5. a, the exact crystalline structure of the sample confirmed by XRD revealed the formation of hydroxyapatite phase (sample S_0) and yielded reflections from (002), (210), (211), (202), (310), (311), (113), (222) and (213) planes. All the samples exhibited almost similar diffraction pattern with characteristic peaks of HA [32]. This crystallographic structure of the biocomposite was more similar to natural bone mineral (biological apatite) ($S_0, S_{0.1}, S_{0.2}, S_{0.4}$ and $S_{0.8}$) [33]. Hence, the HA nanocrystallites in the CA-PAAc/HA nanocomposite have more similarities with natural bone mineral in terms of the degree of crystallinity [34].

From fig. 5 the reflections at 39.4° correspond to the (111) plane of elemental Ag as shown in all samples except S_0 . The diffraction patterns of all samples after 14 days incubation in the SBF solution showed two sharp and clear peaks at 31.8 and 46.5° corresponding to (211) and (222) main reflection planes of apatite-like calcium phosphate (JCPDS No. 09-0432) as shown in Fig. 2(b). The XRD data clearly confirmed that apatite also formed on B_0 (silver free) biocomposite. However, the peaks of ($B_{0.1}, B_{0.2}, B_{0.4}$ and $B_{0.8}$) biocomposite after incubation in the SBF solution were sharper and stronger suggesting that an apatitic compound was formed with higher levels of crystallinity. This result indicates that the incorporation of Ag nanoparticles rapidly accelerates the apatite formation in the biocomposite samples.

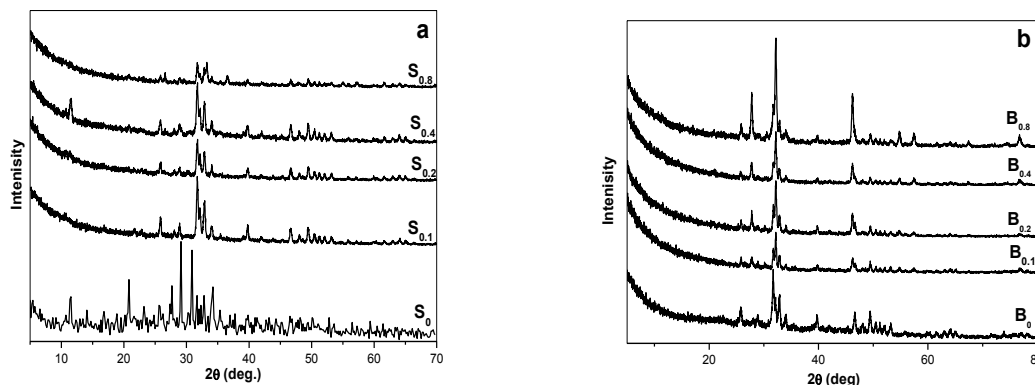


Figure 5: XRD patterns of the PAAc/Cs-HA biocomposite with different concentrations of silver nitrate a) before and b) after soaking in SBF solution

Thermo gravimetric analysis (TGA)

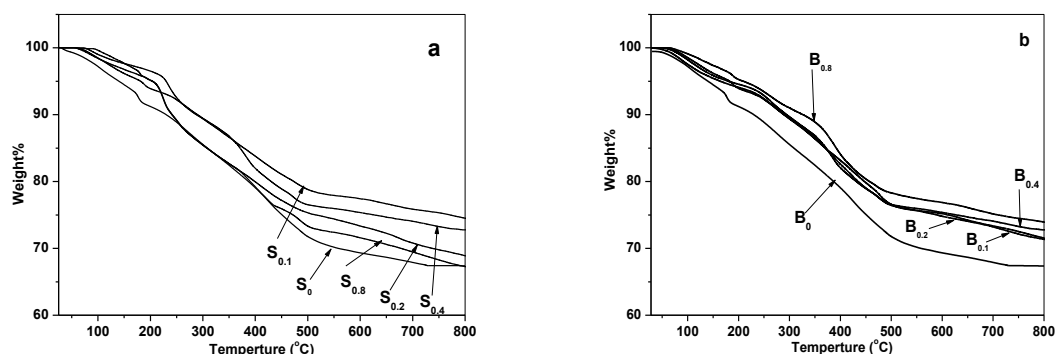


Figure 6: XRD patterns of the PAAC/Cs-HA biocomposite with different concentrations of silver nitrate a) before and b) after soaking in SBF solution

TGA analyses were performed to confirm the formation of apatite-like materials in the PAAC/Cs-HA and PAAC/Cs-HA-Ag biocomposite upon incubation in the SBF solution. Fig. 6a and Fig. 6b shows the TGA analyses of S and B biocomposites samples before and after incubation in the SBF solution, respectively. The TGA results showed that the polymer matrix decomposed in a single step. The decomposition of the composites was found to be in the range of 200– 500 °C before and after 14 days incubation in the SBF solution. From the TGA analysis it was observed that the biocomposite samples after incubation in SBF solution showed higher residual weights than those before incubation.

Furthermore, the residual weight dramatically increases with the addition of Ag nanoparticles in the PAAC/Cs-HA samples as shown in Fig. 6b. This result clearly confirmed that the nucleation effect was increased with addition of Ag nanoparticles in the biocomposite materials. This is because; the incorporation of Ag nanoparticles can enhance the bioactivity of the samples and acted as a heterogeneous nucleating agent which increase its potential use as scaffold for bone tissue engineering application[35]. Also the presence of Ag nanoparticles in biocomposite materials accelerates the formation of apatite aggregation during incubation in the SBF solution. Development of the apatite-like materials on the biocomposite surface depends on the presence of nucleation sites and sufficient concentration of ionic species necessary to form the apatite. Relatively high specific surface area of the rugged Ag nanoparticles on the surfaces of the PAAC/Cs-HA-Ag biocomposites provides the nucleation sites for apatite in SBF compared with PAAC/Cs-HA, results in more energetic nucleation sites. The TGA data is in fair agreement with the SEM results.

CONCLUSIONS

Homogeneous PAAC/Cs-HA biocomposites were fabricated through in situ precipitation method. The addition of Ag nanoparticles in the PAAC/Cs matrix greatly influenced the nucleation and the growth of apatite-like crystal in the biocomposite surface after incubation in SBF. FT-IR and XRD analysis suggested that the apatite formed on the surface of composite in SBF was carbonated apatite, which is similar in composition and structure to bone apatite and increased with the incorporation Ag nanoparticles in the biocomposites. From the TGA analysis it was observed that the PAAC/Cs-HA-Ag biocomposite samples after incubation in SBF solution showed higher thermal stability than PAAC/Cs-HA biocomposite samples. All the above results indicate Ag nanoparticles can enhance the bioactivity of the samples and acted as a heterogeneous nucleating agent which increase its potential use as scaffold for bone tissue engineering application and may further enhance the understanding of biomineralization and shed light on the development of new biomaterials for bone tissue engineering.

REFERENCES

- [1] Rose FR, Oreffo RO. Biochemical and biophysical research communications 2002;292:1-7.
- [2] Du C, Cui F, Zhang W, Feng Q, Zhu X, De Groot K. Journal of biomedical materials research 2000;50:518-527.
- [3] Kikuchi M, Itoh S, Ichinose S, Shinomiya K, Tanaka J. Biomaterials 2001;22:1705-1711.
- [4] Ahmad Z, Mark J. Materials Science and Engineering: C 1998;6:183-196.

- [5] Sailaja G, Velayudhan S, Sunny M, Sreenivasan K, Varma H, Ramesh P. *Journal of Materials Science* 2003;38:3653-3662.
- [6] Li Z, Yubao L, Aiping Y, Xuelin P, Xuejiang W, Xiang Z. *Journal of Materials Science: Materials in Medicine* 2005;16:213-219.
- [7] TenHuisen KS, Martin RI, Klimkiewicz M, Brown PW. *J Biomed Mater Res* 1995;29:803-810.
- [8] Bonfield W. *Ann N Y Acad Sci* 1988;523:173-177.
- [9] Miyazaki S, Ishii K, Nadai T. *Chemical & pharmaceutical bulletin* 1981;29:3067-3069.
- [10] Madihally SV, Matthew HW. *Biomaterials* 1999;20:1133-1142.
- [11] Zhang Y, Zhang M. *Journal of biomedical materials research* 2001;55:304-312.
- [12] Ito M, Hidaka Y, Nakajima M, Yagasaki H, Kafrawy A. *Journal of biomedical materials research* 1999;45:204-208.
- [13] Wang H, Ki W, Lu Y, Wang Z. *J Appl Poly Sci* 1997;65:1445-1450.
- [14] Ahn JS, Choi HK, Cho CS. *Biomaterials* 2001;22:923-928.
- [15] Moharram MA, Balloomal LS, Elgendy HM. *ibid* 1996;59:987-990.
- [16] El-Bahy GS, Abdelrazek EM, Allam MA, Hezma AM. *Journal of Applied Polymer Science* 2010;122:3270-3276.
- [17] Khan MAM, Kumar S, Ahamed M, Alrokayan SA, AlSalhi MS. *Nanoscale research letters* 2011;6:1-8.
- [18] Cengiz B, Gokce Y. *Colloids and Surfaces* 2008;322 29-33.
- [19] Anee TK, Ashok M, Palanichamy M, Kalkura SN. *Mater Chem Phys* 2003;80:725 -730.
- [20] Liu Y, Hou D, Wang G. *Mater Chem Phys* 2004;86:69-73.
- [21] Katti SK. *J of Amer Bioch and Biotech* 2006;2:73-79.
- [22] Lei C, Liao Y, Feng Z. *Biomed Mater* 2009;4:35010.
- [23] Abdelrazek EM, ElDamrawi G, Al-Shahawy A. *Physica B* 2010; 405:808-816.
- [24] Ripamonti U, Duneas N. *MRS Bull* 1996;21:36.
- [25] Wu Y, Guo J, Yang W, Wang C, Fu S. *Polymer* 2006;47:8.
- [26] Wu Y, Guo J, Yang W, Wang C, Fu S. *Polymer* 2006;47:5287-5294.
- [27] Mallikarjuna K, Narasimha G, Dillip G, Praveen B, Shreedhar B, Lakshmi CS, et al. *Digest Journal of Nanomaterials and Biostructures* 2011;6:181-186.
- [28] Yang F, Both SK, Yang X, Walboomers XF, Jansen JA. *Acta biomaterialia* 2009;5:3295-3304.
- [29] [Koutsopoulos S. *Journal of biomedical materials research* 2002;62:600-612.
- [30] Müller L, Müller FA. *Acta Biomaterialia* 2006;2:181-189.
- [31] Li P, Ohtsuki C, Kokubo T, Nakanishi K, Soga N, de Groot K.J *Biomed Mater Res* 1994;28:7-15.
- [32] Abdel-Aziz MS, Hezma A. *Polymer-Plastics Technology and Engineering* 2013;52:1503-1509.
- [33] Jia WT, Zhang X, Luo SH, Liu X, Huang WH, Rahaman MN, et al. *Acta Biomater* 2010;6:812-819.
- [34] Elliot JC. *Structure*, Amsterdam: Elsevier Science 1994;vol. 111.
- [35] Suwantong O, Opanasopit P, Ruktanonchai U, Supaphol P. *Polymer* 2007;48:7546-7557.